JOURNAL OF MATERIALS SCIENCE 19 (1984) 3987–3994

A structural investigation of stabilized oxygen evolution catalysts

R. HUTCHINGS*, K. MÜLLER, KÖTZ, S. STUCKI
Brown Boveri Research Center, CH-5405 Baden, Switzerland

A ternary mixed oxide containing SnO_2, RuO_2 and IrO_2 was shown to exhibit a more stable electrocatalytic behaviour than simpler catalysts consisting of noble metal oxides only. X-ray diffraction and transmission electron microscopy were used to characterize the structure of these oxide catalysts. It was found that precipitation of the fine catalyst powders resulted in the formation of a mixed (Sn, Ru, Ir)O_2 rutile phase. This phase was shown to be thermodynamically unstable, decomposing to SnO_2 and (Ru, Ir)O_2 on annealing at 800° C. X-ray photoelectron spectroscopy revealed that the surface composition of these mixed oxide catalysts varies considerably from the bulk composition. The formation of such metastable, mixed oxides is discussed.

1. Introduction

In recent years an interesting group of new catalysts based upon the oxides of the noble metals, in particular ruthenium and iridium, has emerged. RuO_2 and, to a slightly lesser extent, IrO_2 have been shown [1–3] to possess high catalytic activities in electrochemical reactions, a fact which has been linked to the good metallic conductivity of these oxides [4]. One specific application of such catalysts has been in the development of advanced solid polymer electrolyte (SPE) water electrolysers. In addition to a high activity, the oxygen evolution catalyst in a modern SPE electrolyser must have long-term stability. This has led to the development of mixed (Ru, Ir)O_2 catalysts which provide for optimization of the high activity of RuO_2 and the better stability of IrO_2 [5]. Alternatively, RuO_2 has been studied in combination with base-metal oxides, particularly TiO_2 [6].

In the present paper initial results for the accelerated life testing of mixed oxide catalysts containing RuO_2, IrO_2 and SnO_2 are presented. However, the major aim of the paper is to elucidate the microstructure of these mixed oxides in order to provide the basis necessary for the interpretation of more extensive electrochemical investigations. The microstructure of a number of mixed oxides, prepared by thermal decomposition of appropriate mixtures of the corresponding chlorides, was studied by X-ray diffraction, analytical electron microscopy and X-ray photoelectron spectroscopy (XPS). These techniques were used as they provide a clear picture of the chemical and crystallographic homogeneity of the catalysts. In addition to studying the effects of the preparation technique, the thermal stability of the microstructure was also studied. The results obtained are discussed with reference to those from previous structural investigations of binary and ternary mixed oxides based on ruthenium or iridium dioxide.

2. Experimental procedure

The starting materials used to prepare the oxide catalysts were $SnCl_2$ (Fluka analytically pure grade), $RuCl_3 \cdot xH_2O$ (Degussa 36.55% metal content) and $H_2IrCl_6 \cdot xH_2O$ (Degussa 38.5% metal content). The oxide powders were produced by vacuum evaporation followed by either firing in air or processing by a modified Adams [7] salt-melt technique. Individual starting materials were dissolved in 2-propanol. Suitable proportions of these solutions were then mixed and vacuum-evaporated to near dryness in a rotating, round-bottom flask. The residue was then fully dried

*Present address: Department of Metallurgy and Materials Science, University of Cape Town, Rondebosch 7700, RSA.

0022–2461/84 $03.00 + .12

in vacuum at a temperature of approximately 100° C. In the case of the air-fired material a final, stabilizing heat-treatment was carried out by firing for 3 h at 450° C. For the Adams technique, the dried residue from the vacuum evaporation treatment was mixed with an excess of sodium nitrate. The mixture was then fused and held at 450° C for 3 h. This fused mixture constitutes an oxidizing melt which produces precipitation of the mixed metal oxides. After cooling, the salt was dissolved in hot water and the oxide was obtained by filtering, washing and drying. Brunauer–Emmett–Teller (BET) analysis [8] indicated that the powder produced by both techniques was extremely fine, with specific surface areas in the range 30 to 150 $m^2 g^{-1}$.

For the accelerated life testing the catalyst was coated onto porous, lightly platinized, titanium sheet (with a loading of approximately 5 mg cm^{-2}). The coating process entailed making a paste from the catalyst, polyvinylidene fluoride (PVDF) powder and dimethyl formamide. This paste is painted onto the electrode and dried at 250° C so that the PVDF acts as a binder for the catalyst. The performance of the coated electrode was then evaluated, with respect to oxygen evaluation, in a standard H-type cell [9] (two compartments for anode and cathode joined by a channel, to avoid gas intermixing, and an external reference electrode with Luggin capillary reaching close to the anode); a platinum wire was the counter-electrode. The electrolyte was 6N H_2SO_4 and the cell temperature approximately 50° C. The cell was operated continuously at an anodic current density of 1 A cm^{-2}. The operating potential of the anode was periodically measured against a reference electrode. During measurement the current was temporarily reduced to 0.1 A cm^{-2} in order to reduce the ohmic error in the potential reading.

The XPS measurements were performed with a Kratos ES 300 electron spectrometer using non-monochromated Mg$K\alpha$ radiation. The instrumental resolution was 1.2 eV FWHM, measured at the Au $4f_{7/2}$ line. The electron analyser was operated in the fixed-retarding-ratio mode, which provides a sensitivity proportional to the kinetic energy of the photoelectrons. Specimens were prepared by lightly pressing the oxide powders into copper foil. Conductivity of the oxides was adequate to prevent any problems due to charging of the specimen.

X-ray diffraction measurements were made on a Guinier–De Wolf camera (Enraf-Nonius) with a quartz crystal monochromator and using Cu$K\alpha$ radiation. All electron microscopy was performed on a Jeol 200CX microscope with a Link Systems 860 Series 2 energy-dispersive X-ray analysis unit. Specimens for the electron microscopy were prepared by dispersion from aqueous suspension onto a carbon film supported on a copper grid.

3. Results

3.1. Accelerated life tests

Four oxide catalysts, all of the air-fired type, were subjected to an accelerated life test. These oxides were pure RuO_2, pure IrO_2, a binary mixed oxide $(Ru_{0.5}Ir_{0.5})O_2$ and a ternary mixed oxide $(Sn_{0.5}Ru_{0.25}Ir_{0.25})O_2$. The results for the last three are summarized in Fig. 1. Using the curve for IrO_2 as a reference, one can see that the binary mixed oxide, curve 2, is more active (i.e. the potential for oxygen evolution at 0.1 A cm^{-2} is lower) but has a comparable life time as indicated by the sharp upturn at around 800 h. The ternary mixed oxide, curve 3, shows an initially lower activity, but a much improved stability which results in superior behaviour to that of the IrO_2 and $Ru_{0.5}Ir_{0.5}O_2$ at test lives of 320 and 730 h, respectively. The data for pure RuO_2 are not shown in Fig. 1 owing to the highly unstable behaviour of this catalyst, which could be represented by a line drawn vertically from the origin of the graph shown in Fig. 1.

3.2. Microchemistry and microstructure of $(Ru_x Ir_{1-x})O_2$ type catalysts

XPS was first performed on a range of binary mixed oxides. The relative surface compositions

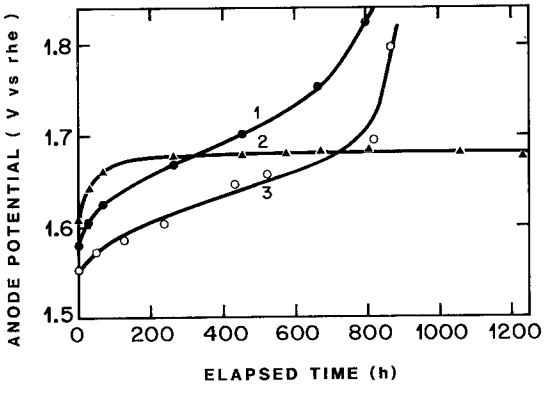

Figure 1 The variation of the anode potential with time during the accelerated life testing of three oxide catalysts. 1 – IrO_2; 2 – $(Ru_{0.5}Ir_{0.5})O_2$; 3 – $(Sn_{0.5}Ru_{0.25}Ir_{0.25})O_2$.

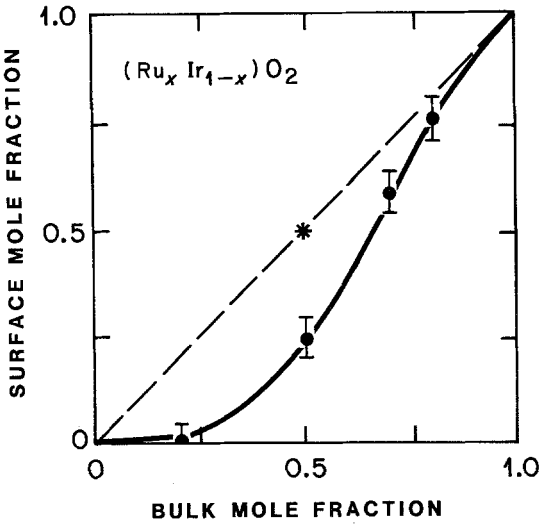

Figure 2 XPS results for the surface composition of a range of (Ru, Ir)O_2 powders as a function of the bulk composition. (The asterisk indicates the analysis of an equimolar, physical mixture of the component oxides.)

were determined for a range of oxides of the general formula $(Ru_xIr_{1-x})O_2$, where x varied between 0 and 1. Compositions were calculated from the peak areas for the Ru $3d_{5/2}$, Ir $4f_{7/2}$ and O 1s emission levels. Corrections were made for the energy dependence of the analyser transmission and the subshell photoionization cross-sections as tabulated in the literature [10]. The escape depth for the emitted electrons was assumed to be independent of composition. This procedure was checked by analysis of physical mixtures of the oxides, and was found to be accurate to within ± 5 per cent.

The data obtained for a range of binary mixed oxides prepared by the modified Adams technique are shown in Fig. 2. As the sampling depth for XPS is in the order of 2 nm, it is clear from the data in Fig. 2 that the surface of the catalyst powder is enriched in iridium.

The X-ray diffraction pattern obtained from a $(Ru_{0.5}Ir_{0.5})O_2$ catalyst showed very broad, weak lines indicative of an extremely fine powder with the tetragonal, rutile, crystal structure. The lines were much too broad to accurately determine the lattice parameters for the mixed oxide. Electron diffraction gave much sharper rings, confirming the rutile structure, but the technique lacks the inherent precision to differentiate between the lattice parameters of a true mixed oxide and the two end components, RuO_2 and IrO_2 (for which the parameters are shown in Table I). However, energy dispersive X-ray (EDX) analysis did indicate that the ruthenium and iridium were certainly intermixed at a spatial resolution of 50 nm.

Imaging the powder by transmission electron microscopy revealed the crystallite size to be in the range 3 to 10 nm. The mean particle size, $\bar{d}$, may be related approximately to the surface area, A, and the volume, V, of the powder according to the simple formula [13],

$$\bar{d} = 6V/A \quad (1)$$

Equation 1 may be directly rewritten in terms of the specific area, S, and the density, ρ, as follows:

$$\bar{d} = 6/S\rho \quad (2)$$

Assuming a density of 9.4 g cm^{-3} for $(Ru_{0.5}Ir_{0.5})O_2$, a mean particle diameter of 5 nm is seen to correspond to a specific surface area of 130 $m^2 g^{-1}$. Hence the observed crystallite size is in good agreement with the BET measurements mentioned earlier.

3.3. Microstructural analysis of $(Sn_{1-2x}Ru_xIr_x)O_2$ type catalysts produced by firing in air

Ternary mixed oxides were produced by combining various proportions of SnO_2 with equimolar amounts of RuO_2 and IrO_2. In the case of the catalysts produced by firing in air, X-ray diffraction indicated a considerable degree of heterogeneity. Fig. 3 shows a microdensitometer trace across the (1 1 0) and (1 0 1) reflections of an as-prepared oxide with the nominal composition $(Sn_{0.5}Ru_{0.25}Ir_{0.25})O_2$, compared with that from the same material after heating to 800° C for 24 h. The as-prepared material (dotted line) exhibited two sets of diffraction lines, a sharp set corresponding to the rutile structure of SnO_2 and a much broader set corresponding to (Ru, Ir)O_2 but displaced slightly to lower values of two theta. The diffraction line positions were calibrated with reference to a KCl standard.

Electron microscopy confirmed that this catalyst consisted of a mixture of relatively large particles around 1 μm in size and much finer, 5 to 10 nm particle size, powder. EDX analysis and electron diffraction confirmed the large particles to be essentially pure SnO_2, whereas the fine powder was seen to be (Ru, Ir)O_2 containing various amounts of tin. The incorporation of the tin into the mixed oxide was evidenced by both EDX

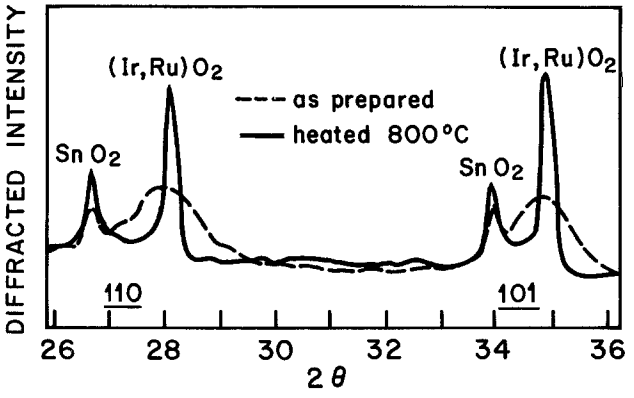

Figure 3 Microdensitometer traces across the (1 1 0) and (1 0 1) reflections of X-ray diffraction patterns obtained from an air-fired $(Sn_{0.5}Ru_{0.25}Ir_{0.25})O_2$ catalyst before and after heat treatment at 800° C.

analysis and an increase in the lattice parameter determined by electron diffraction. The electron diffraction data were calibrated with reference to thallous chloride.

As will be discussed later, SnO_2 is not expected to be mutually soluble with RuO_2 and IrO_2. In view of this fact, the catalyst was heated to 800° C to check the stability of the ternary mixed oxide. The full line in Fig. 3 represents the heat-treated material. It can be seen that the $(Ru, Ir)O_2$ peaks have sharpened and shifted back to their expected positions. This suggests an increase in particle size and rejection of the SnO_2 from solution, both of which were confirmed by electron microscopy.

3.4. Microstructural analysis of $(Sn_{1-2x}Ru_xIr_x)O_2$ type catalysts produced by the Adams technique

The ternary mixed oxides made by the modified Adams process were found to be much more homogeneous than the air-fired material. X-ray diffraction patterns obtained from material containing nominally 20, 50 and 80 mol% of SnO_2 showed a single set of very broad lines corresponding to the rutile structure. Lattice parameter determination was impossible due to the extreme width, and flatness, of these peaks.

Transmission electron microscopy (TEM) revealed the Adams catalysts to be morphologically homogeneous, see Fig. 4. EDX analysis and electron diffraction again confirmed that the SnO_2 was thoroughly intermixed with the $(Ru, Ir)O_2$, as was the case for the finer portion of the air-fired powder. However, detailed investigation revealed that the local tin concentration varied as much as 20 mol% from the nominal composition. In order to study this effect more carefully, EDX and diffraction analyses were carried out on a number of areas on a range of specimens. In this way the correlation between composition and lattice parameter could be checked.

For the purpose of quantification of the EDX

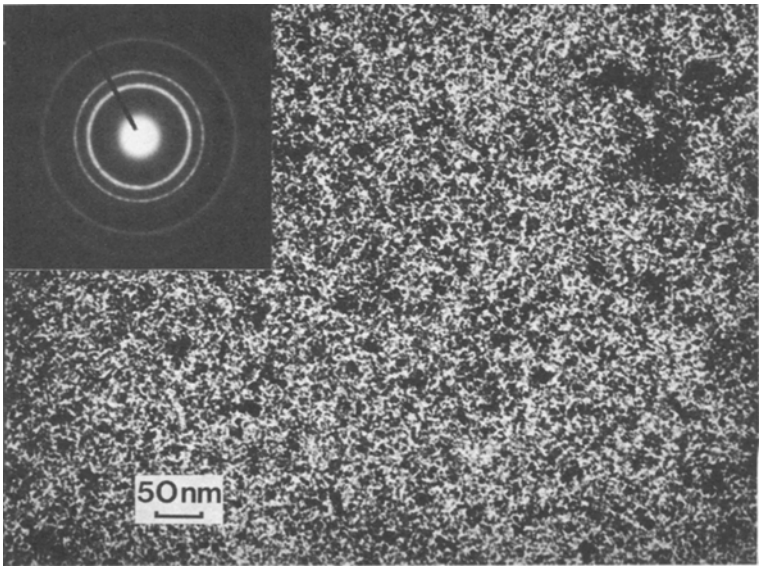

Figure 4 TEM micrograph of a $(Sn_{0.8}Ru_{0.1}Ir_{0.1})O_2$ catalyst as prepared by the modified Adams process. The inset shows a selected-area diffraction pattern taken with 1 μm diameter aperture.

TABLE I Lattice parameters for the pure oxides (mean values from [11] and [12])

	IrO_2	RuO_2	SnO_2
a (nm)	0.450	0.450	0.474
c (nm)	0.311	0.314	0.319

data, the relative areas of the SnL, RuL and IrM peaks were corrected using calculated sensitivity factors [14]. In view of the thin nature of the dispersed catalysts, and the proximity of the three peaks of interest, no correction was made for absorption. Analysis of a physical mixture containing equimolar proportions of SnO_2, RuO_2 and IrO_2 indicated that this procedure was accurate to within 10%. Inspection of the lattice parameter values listed in Table I shows that the "a" parameter is most suitable for monitoring any change from the (Ru, Ir)O_2 structure towards that of SnO_2. Accordingly, Fig. 5 gives a graphical representation of the experimentally determined relationship between lattice parameter and composition, from which it can be seen that the "a" parameter is reasonably well correlated to the mole fraction of SnO_2.

As was true for the air-fired (Sn, Ru, Ir)O_2 catalysts, heating to 800° C for 24 h resulted in particle coarsening and separation of the mixed oxide into two components, namely SnO_2 and (Ru, Ir)O_2. The effect of this heat treatment upon the morphology of the oxides is clearly illustrated in Fig. 6. The diffraction pattern reveals this to be an area composed mainly of (Ru, Ir)O_2, with a little SnO_2 giving rise to the spots just inside the main rings.

In view of the surface segregation described in Section 3.1, XPS analysis was carried out on Adams material containing $(Sn_{0.5}Ru_{0.25}Ir_{0.25})O_2$. The evolution of the surface chemistry as a result of subsequent heat treatment was also studied. Quantification was performed as described earlier, using the Sn $3d_{5/2}$ peak to estimate the tin content. The results are summarized in Fig. 7. As for the binary mixed oxides the surface of the as-prepared material was found to be enriched in iridium with respect to ruthenium. In addition, the surface was seen to be highly depleted in tin. Annealing at progressively higher temperatures was observed to shift the surface composition closer to that of the bulk.

4. Discussion

4.1. The binary oxide system RuO_2–IrO_2

The structural analysis of the binary mixed oxides, as described in Section 3.2, clearly shows that mixed oxide catalysts of the form (Ru, Ir)O_2 can be produced with a very fine grain size. The observation of mutual solubility for the oxides RuO_2 and IrO_2 is not new. McDaniel and Schneider [15] reported a continuous range of solid solubility for the system RuO_2–IrO_2, based upon results from the high temperature reaction of the component oxides. More recently, Georg and co-workers [16] have successfully grown, by vapour transport,

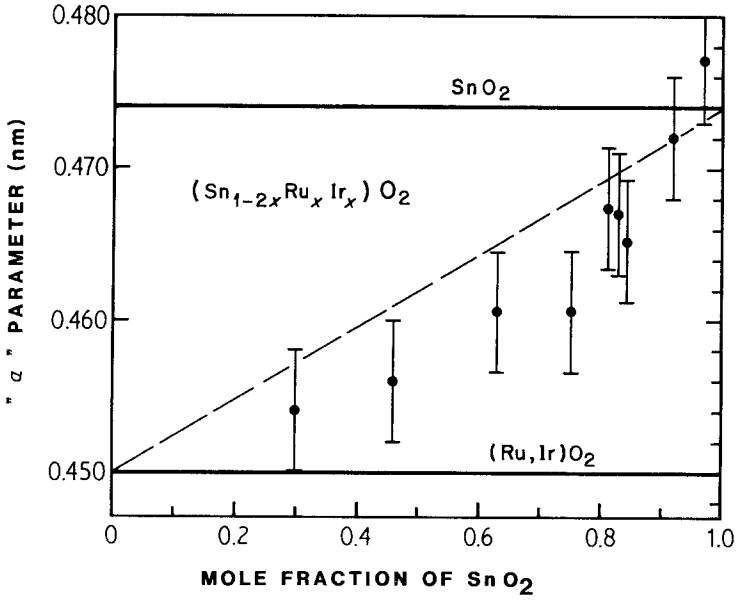

Figure 5 Variation of the "a" parameter as a function of SnO_2 content for (Sn, Ru, Ir)O_2.

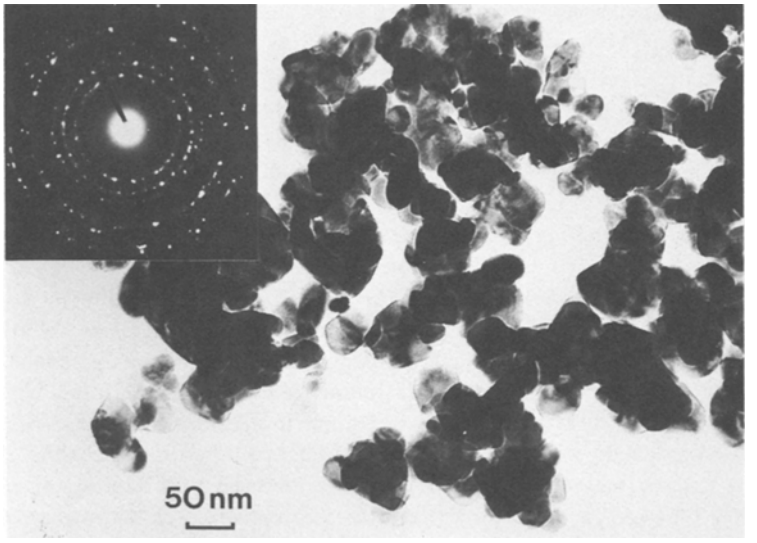

Figure 6 TEM micrograph and selected-area diffraction pattern from a (Sn, Ru, Ir)O_2 catalyst after heating at 800° C for 24 h.

single crystals at a number of points in the (Ru, Ir)O_2 phase field.

However, although the observation of mutual solubility is not new, it is worthwhile considering why this solubility occurs, before moving on to the more complex SnO_2–RuO_2–IrO_2 system. Both RuO_2 and IrO_2 have the rutile structure, hence substitution provides the obvious means for mutual dissolution. The major parameter determining whether substitution may occur on the cation sublattice is the ionic radius [17]. For the Ru^{4+} and Ir^{4+} ions, the effective radii are 0.076 and 0.077 nm, respectively [18]. Thus, substitution is favourable. A second parameter of importance is the nature of bonding, as will be discussed in the next section. However, Ru^{4+} and Ir^{4+} ions in the rutile structure both exhibit some degree of delocalization of the outer electrons giving rise to metallic bonding [19], therefore providing no obstacle to direct substitution.

The above discussion leads to the conclusion that mutual solubility of RuO_2 and IrO_2 is perfectly reasonable. Therefore, it is of interest to consider the significance of the XPS data. Two possible explanations exist for the observed enrichment of iridium at the surface. On one hand, the larger size of the Ir^{4+} ion may be responsible for its segregation to the surface, where the necessary expansion is more easily accommodated. This possibility is particularly intriguing because the maximum in deviation from the bulk composition, Fig. 2, falls in the same compositional range as the

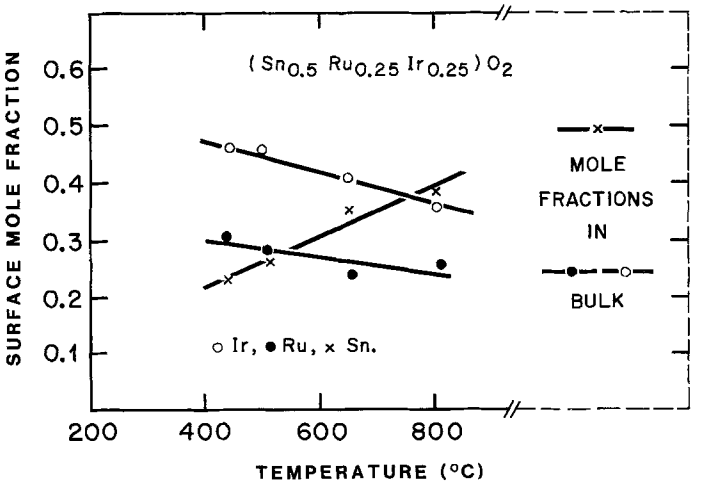

Figure 7 XPS results for the surface composition of the (Sn, Ru, Ir)O_2 catalyst as a function of annealing temperature.

maximum deviation from Vegard's law seen in the previously reported X-ray data [15, 16]. However, it is equally likely that the XPS data can be explained simply in terms of the higher oxidation potential of the ruthenium leading to a ruthenium enrichment during the earlier stages of crystal growth, and hence a ruthenium deficiency in the later stages. It is not possible to distinguish between these two mechanisms on the basis of the available data.

4.2. The ternary oxide system SnO_2–RuO_2–IrO_2

The main feature of interest in the ternary oxide catalysts is the extensive intermixing observed between the SnO_2 and the $(Ru, Ir)O_2$. Although no data exist in the literature for this ternary system, two previous studies have shown only restricted solid solution in the system SnO_2–IrO_2. On the basis of high temperature reaction of the constituent powders, McDaniel and Schneider [20] showed no detectable solubility of IrO_2 in SnO_2, and a solubility limit of about 2 mol% for SnO_2 in IrO_2 at 1000° C. Secondly, Reames [21], whilst attempting to grow SnO_2 crystals containing 10 mol% IrO_2, found a maximum of 0.1% in solution. Hence, formation of a $(Sn, Ru, Ir)O_2$ phase is certainly not expected from previous data. From the more theoretical viewpoint, the ionic radius of Sn^{4+}, at 0.083 nm, is considerably larger than those of Ru^{4+} and Ir^{4+}. However, it still lies just within the Hume-Rothery limit for successful substitution. The reason for the metastable nature of the $(Sn, Ru, Ir)O_2$, as evidenced by the separation upon heating at 800° C, must therefore lie elsewhere. The prime candidate is the very different electronic configuration of the Sn^{4+} ion. Whereas RuO_2 and IrO_2 are both metallic conductors, SnO_2 is a wide-gap semiconductor. In this way SnO_2 (band gap ~ 3.5 eV) may be regarded as being comparable to TiO_2 (band gap ~ 3.05 eV), which is also known to demonstrate only limited solid solubility, at moderate temperatures, with RuO_2 [22] and IrO_2 [20]. So, it would seem that it is the large difference in the nature of the bonding which prevents the formation of a stable mixed oxide.

It is interesting to consider, how intimate is the mixing of the cations. For instance, Triggs *et al.* [23] have shown that single crystals of $(Ti, Ru)O_2$, grown by vapour transport, are really composed of very fine platelets of RuO_2 in a TiO_2 matrix. Similarly, Roginskaya and colleages [6, 24] have proposed that interconnecting clusters of RuO_2 are present in $(Ru, Ti)O_2$ catalysts. On the basis of the present results it is clear that the $(Sn, Ru, Ir)O_2$ material is not simply a mixture of fine crystals of SnO_2 and $(Ru, Ir)O_2$, but some clustering may occur and it is not possible to rule out the models suggested above.

The next question to be looked at is that of why intermixing was observed under the present conditions but not in the experiments of McDaniel and Schneider [20], and Reames [21]. An answer to this question is suggested by the XPS results shown in Fig. 7. In the as-prepared condition (450° C), when the $(Sn, Ru, Ir)O_2$ phase is present, the XPS data show a large deficiency in tin at the surface. As discussed in Section 4.1, the larger Sn^{4+} ion would be expected to segregate to the surface. Thus, its deficiency at the surface seems to indicate that it is the kinetics of precipitation that produces the observed difference between bulk and surface composition. (This is consistent with surface composition shifting towards that of the bulk with higher heat treatment temperatures.) It is therefore hypothesized that the fortuitously controlled precipitation kinetics are responsible for producing the mixed $(Sn, Ir, Ru)O_2$ catalyst. Further, in view of the superior homogeneity of the Adams catalysts, the modified Adams technique appears to result in a more controlled precipitation. This would seem to be reasonable in view of the more homogeneous dispersion, the better temperature control and the faster reaction rates associated with the Adams-type process.

4.3. Catalytic behaviour of the mixed oxide

The accelerated life tests clearly show that the good properties of RuO_2 and IrO_2 may be combined to some extent. In addition, the introduction of SnO_2, a base-metal oxide, is seen to alter the behaviour in a significant fashion. This change appears to be associated with the SnO_2 being incorporated into the $(Ru, Ir)O_2$ structure. It should be pointed out that these tests were carried out on the earlier, air-fired specimens, not the more homogeneous material produced by the modified Adams process. Hence, a more extensive investigation of the catalytic behaviour of the variously treated materials would be needed to fully evaluate the significance of the structure of the catalyst. At the moment it can be said only that it will be necessary to consider the complex

electronic structure of an intermixed (Sn, Ru, Ir)O_2 phase, the basic characteristics of which have been identified by the present work.

5. Conclusions

In summary, it may be stated that a catalyst containing a mixture of SnO_2, RuO_2 and IrO_2 was seen to exhibit superior electrochemical stability to that of a mixed (Ru, Ir)O_2 catalyst. This behaviour is associated with the formation of a thermodynamically metastable phase of the form (Sn, Ru, Ir)O_2 with the rutile structure.

Acknowledgements

The authors are grateful to Mrs R. Loitzl for careful preparation of the catalysts, and to Brown Boveri and Co. for granting permission to publish this article.

References

1. D. GALIZZIOLI, F. TANTARDINI and S. TRASATTI, *J. Appl. Electrochem.* **4** (1974) 57.
2. *Idem, ibid.* **5** (1975) 203.
3. J. HORKANS and M. W. SHAFER, *J. Electrochem. Soc.* **124** (1977) 1202.
4. W. D. RYDEN, A. W. LAWSON and C. C. SARTAIN, *Phys. Rev. B* **1** (1970) 1494.
5. S. STUCKI and R. MÜLLER, in "Hydrogen Energy Progress", Proceedings of the 3rd World Hydrogen Energy Conference, Tokyo, 1980, edited by T. N. Veziroglu, K. Fueki and T. Ohta (Pergamon Press, Oxford, 1981) p. 1799.
6. Yu. E. ROGINSKAYA, V. I. BYSTROV and D. M. SHUB, *Zh. Neorg. Khim.* **22** (1977) 201.
7. R. ADAMS and R. L. SHRINER, *J. Amer. Chem. Soc.* **45** (1923) 2171.
8. J. M. THOMAS and W. J. THOMAS, "Introduction to the Principles of Heterogeneous Catalysis" (Academic Press, London, 1967) p. 82.
9. See, for example, D. A. McINNES, "The Principles of Electrochemistry" (Dover Publications, New York, 1961) pp. 109, 454.
10. M. CARDONA and L. LEY, in "Topics in Applied Physics", Vol. 26: "Photoemission in Solids I", edited by M. Cardona and L. Ley (Springer, New York, 1978) p. 82.
11. G. V. SAMSONOV, "The Oxide Handbook" (IFI/Plenum, New York, 1973).
12. W. B. PEARSON, "A Handbook of Lattice Spacings and Structures of Metals and Alloys", Vol. 1 (Pergamon, Oxford, 1958).
13. J. R. ANDERSON, "Structure of Metallic Catalysts" (Academic Press, London, 1975) p. 364.
14. P. J. STATHAM, in "Energy Dispersive X-ray Spectrometry", edited by K. F. J. Heinrich *et al.* (NBS Special Publication 604, Washington D.C., 1979).
15. C. L. McDANIEL and S. J. SCHNEIDER, *J. Res. NBS* **73A** (1969) 213.
16. C. A. GEORG, P. TRIGGS and F. LÉVY, *Mater. Res. Bull.* **17** (1982) 105.
17. O. MULLER and R. ROY, "The Major Ternary Structural Families" (Springer Verlag, Berlin, 1974) p. 11.
18. R. D. SHANNON and C. T. PREWITT, *Acta Crystallogr.* **B25** (1969) 925.
19. J. B. GOODENOUGH, in "Progress in Solid State Chemistry", Vol. 5, edited by H. Reiss (Pergamon Press, Oxford, 1971) p. 145.
20. (a) C. L. McDANIEL and S. J. SCHNEIDER, *J. Res. NBS* **71A** (1967) 119; (b) E. N. BALKO and C. R. DAVIDSON, *J. Inorg. Nucl. Chem.* **42** (1980) 1778.
21. F. M. REAMES, *Mater. Res. Bull.* **11** (1976) 1091.
22. W. O. GERRARD and B. C. H. STEELE, *J. Appl. Electrochem.* 8 (1978) 417.
23. P. TRIGGS, H. BERGER, C. A. GEORG and F. LÉVY, *Mater. Res. Bull.* **18** (1983) 677.
24. Yu. E. ROGINSKAYA, B. Sh. GALYAMOV, I. D. BELOVA, R. R. SHIFRINA, V. B. KOZHEVNIKOV and V. I. BYSTROV, *Elektrokhimiya,* **18** (1981) 1327.

Received 29 December 1983
and accepted 2 February 1984